Published in final edited form as:
J Control Release. 2014 March 28; 178: 63–68. doi:10.1016/j.jconrel.2014.01.014.

Hydrogel-nanoparticle composites for optically modulated cancer therapeutic delivery

Laura E. Strong[1], **Shreyas N. Dahotre**[1], and **Jennifer L. West**[1,2,*]

[1]Department of Biomedical Engineering, Duke University, Durham, NC, United States

[2]Department of Mechanical Engineering, Duke University, Durham, NC, United States

Abstract

A poly(N-isopropylacrylamide-co-acrylamide) (NIPAAm-co-AAm) hydrogel with near-infrared (NIR) absorbing silica-gold nanoshells was designed as a platform for pulsatile delivery of cancer therapeutics. This hydrogel was designed to have a lower critical solution temperature (LCST) above physiologic temperature, such that the material will transition from a hydrated state to a collapsed state above ~40 °C. Additionally, the silica-gold nanoshells used were designed to have a peak extinction coefficient in the NIR, where penetration of light through tissue is maximal. This heat-triggered material phase transition of the composite was found to follow exposure of NIR light, indicating the ability of the NIR absorption by the nanoshells to sufficiently drive this transition. The composite material was loaded with either doxorubicin or a DNA duplex (a model nucleic acid therapeutic), two cancer therapeutics with differing physical and chemical properties. Release of both therapeutics was dramatically enhanced by NIR light exposure, causing 2-5x increase in drug release. Drug delivery profiles were influenced by both the molecular size of the drug as well as its chemical properties. The DNA therapeutic showed slower rates of nonspecific delivery by passive diffusion due to its larger size. Additionally, only 70% of the more hydrophobic doxorubicin was released from the material, whereas the more hydrophillic DNA showed over 90% release. Further, hydrogel composites were used to deliver the doxorubicin to CT.26-WT colon carcinoma cells, eliciting a therapeutic response. This work validates the potential application for this material in site-specific cancer therapeutic delivery.

Keywords

Thermally responsive; N-isopropylacrylamide; Nanoparticle; Hydrogel; Cancer therapeutics

*Corresponding author P.O. Box 90281 Durham, NC 27708, United States tel: (919) 660-5458 fax: (919) 684-4488 jennifer.l.west@duke.edu.

1 Introduction

Pulsatile drug release, defined as a rapid release of drug molecules following an off-release period [1], is beneficial for the treatment of a wide range of diseases. For example, in the treatment of hormone disorders and diabetes, a constant plasma drug level is not desirable. Rather, a rapid increase in drug concentration should follow in response to a biologic stimulus [1,2]. Diseases which benefit from chronotherapy, in which a drug administration timing is optimized [3], would also benefit from a pulsatile delivery system. Cancer is an area where advantages of chronotherpay have been widely studied [4].

While great improvements have been made over the past 50 years in the use of chemotherapy to treat cancer, these treatments still often fail to completely cure malignant disease [5]. This is primarily due to cancer cells becoming genetically resistant to anti-cancer drugs, as well as the adverse side effects of these treatments dictating patients' regimens [4]. Chronotherapy can be used to become to overcome some of these problems by optimizing the timing of drug administration with the circadian rhythms of cancer cell susceptibility and those of adverse side effects [4]. For example, in the treatment of metastatic colorectal cancer, it has been shown that administration of chemotherapeutics by chronotherapy is more efficacious than when the same treatment is administered as a constant infusion [6]. Additionally, the lessening of side effects due to chronotherapy also allows for administration of fuller, more effective doses of chemotherapeutics [4]. While these approaches show promise, implementation of such approaches are often logistically difficult, leading to the need for new methods to improve control of such delivery [3].

One approach for the creation of a pulsatile release system employs thermally responsive polymer-nanoparticle composite materials [7]. These composites couple a polymer material with physical properties that are dependent on temperature with nanoparticles that generate heat in response to external stimuli. Commonly, these materials will transition from a hydrated state at lower temperatures and undergo collapse by releasing water when the temperature is raised above a lower critical solution temperature (LCST). These types of materials have been investigated for drug delivery applications, where therapeutic molecules are absorbed into the material and subsequently released as water is expelled from the hydrogel during the phase transition [8].

This study investigates a poly[N-isopropylacrylamide-co-acrylamide] (NIPAAmco-AAm)-gold nanoshell composite material for use in optically triggered cancer therapeutic delivery. Poly(NIPAAm) is a commonly investigated thermally-responsive polymer for biomedical applications, as it has an LCST of 32 °C, which is near the physiologically relevant body temperature for humans [8]. In addition, by polymerizing with a more hydrophillic copolymer, such as acrylamide, the LCST of the material can be raised above 40 °C [9]. A 95:5 molar ratio of NIPAAm:AAm has been shown to result in an LCST above 37 °C, such that the material will be in a swollen state under physiologic conditions, but collapse slightly above body temperature. This allows drug molecules to be absorbed into and constrained within the material until the material deswells due to a temperature increase to above the LCST. This copolymer has been previously used in drug delivery investigations [10,11].

NIPAAm:AAm copolymers can undergo their LCST transition in response to localized heating by encapsulated nanoparticles [10,11]. Gold-silica nanoshells are a class of nanoparticles that consist of a dielectric silica core surrounded by a thin gold shell [12,13]. These particles have a tunable plasmon resonance dependent on the core size and shell thickness [12,13]. As the particles are exposed to wavelengths of light matching their plasmon resonance, an oscillation of conduction band electrons results in dissipation of this light energy as heat [14,15]. Particles that have a plasmon resonance in the near infrared (NIR) range (700-900 nm) are of particular interest for biological applications. This range is above where most biological chromophores absorb light but below wavelengths where water starts to strongly absorb; thus NIR light is easily transmitted through biological tissue resulting in relatively little attenuation or tissue damage [16]. Gold-silica nanoshells with a 120 nm silica core and 10-15 nm gold shell maximally absorb light in the NIR range at approximately 800 nm, and have been previously investigated for use in cancer diagnostics and photothermal therapy [17–21].

This work describes the synthesis and characterization of this composite hydrogel, and then evaluates the ability to load the hydrogels with cancer therapeutics and trigger drug release upon NIR light exposure. We assessed release of two therapeutics: a chemotherapeutic (doxorubicin) and a biologic therapeutic (a DNA duplex targeting EphA2). These are both important cancer therapeutics and also represent opposite ends of the delivery spectrum in terms of molecular size and hydrophobicity. Doxorubicin is a small molecule (580 Da) chemotherapeutic indicated in a wide variety of cancers including hematopoietic malignancies; carcinomas of the breast, lung, ovary, stomach, and thyroid; and sarcomas of bone and soft tissue [22]. The primary mechanism of action is intercalation with DNA during replication, causing inhibition of topoisomerase II binding and arrest of cell replication [23]. Side effects of doxorubicin include myelosuppression, mucositis, and cardiac toxicity; furthermore, these side effects often cause patients to cease doxorubicin therapy, even if the drug is still effective against their malignancy [24].

In addition, delivery of a larger, more hydrophillic molecule was assessed. A short DNA duplex was investigated as a model nucleic acid therapeutic. This dsDNA molecule was designed to be similar in chemical structure to an siRNA therapeutic. Typical siRNAs are double-stranded with sticky ends and molecular weights of 12-15 kDa. This study employed a 21 base pair (12,850.5 kDa) oligonucleotide equivalent in sequence to an siRNA targeting the EphA2 protein (target sequence 5’-AATGACATGCCGATCTACATG-3’) [25]. EphA2 is a receptor tyrosine kinase known to be upregulated in many cancers; its functions include signaling involved in cell-cell contacts, cell migration, and angiogenesis [26]. Down regulation of EphA2 has been shown to reduce tumorigenicity in preclinical studies of several cancer types, including pancreatic and breast carcinomas [27].

2 Materials and methods

All reagents were purchased from Sigma-Aldrich and used as received, unless otherwise noted. All water used in synthesis, purification, and testing was treated by a Milli-Q system (18.2 MΩ·cm resistivity, Millipore).

2.1 Gold-silica nanoshell fabrication

Gold-silica nanoshells, consisting of a silica core surrounded by a thin gold shell, were fabricated based on previous methods. Silica cores 120 nm in diameter (Precision Colloids) were surface-functionalized with amine groups via a reaction with aminopropyltriethoxysilane (Gelest Inc). Colloidal gold was prepared by a reduction of chloroauric acid (Alfa Aesar) as previously described in the literature [28]. The aminated silica cores were then mixed with this gold colloid suspension to adsorb the colloidal gold onto the silica core via electrostatic interactions with the amine groups. These adsorbed colloids then acted as nucleation sites for growth of a continuous gold shell. In this final shell growth step, additional gold was reduced onto the adsorbed gold colloids in a reduction of $HAuCl_4$ by formaldehyde, causing the gold to coalesce to form a continuous shell of ~ 15 nm around the silica core. The extinction characteristics of the particles were analyzed by UV-Vis spectroscopy (400-1100 nm, Cary 50 Varian). Transmission electron microscopy (TEM) (FEI Tecnai G^2 Twin) and dynamic light scattering (DLS) (Malvern Zetasizer Nano ZS) were employed to further characterize and size the resulting particles. Only particles with a polydispersity index (PDI) of <10% were used in subsequent steps.

2.2 Poly(NIPAAm-co-AAm) hydrogel synthesis

Poly(NIPAAm-co-AAm) hydrogels were synthesized by free radical polymerization. Prior to use, NIPAAm (97%, Sigma-Aldrich) was dissolving in tetrahydrofuran (THF) and recrystallized three times in *n*-hexane to remove *p*-methoxylphenol, a polymerization inhibitor present for packaging.

A 1.75 M monomer solution composed of a 95:5 molar ratio of NIPAAm:AAm and a 1:750 molar ratio of monomer:crosslinker (MBAAm) was prepared in H_2O and added to a three-neck round bottom flask (3.75 ml total volume). Argon (Ar) gas was bubbled through this solution for at least 15 min. With rapid stirring, 37.5 μl of 10% (w/v) ammonium persulfate and 7.5 μl of *N*,*N*,*N*′,*N*′-tetramethylethylenediamine were added to initiate polymerization. Composite hydrogels were synthesized in a similar fashion, with 8×10^9 nanoshells/ml added to the monomer solution prior to adding APS/TEMED. This concentration of nanoshells was chosen since previous studies indicate that this concentration should be sufficient to cause enough heating to drive our polymer phase transition [10,11]. The polymerization solution was then quickly poured into a mold consisting of 2 glass slides separated by a 1.5 mm Teflon® spacer held together by metal clamps. The hydrogel was cured at 30 °C for 2 h under vacuum. After curing, the hydrogel slab was soaked in 95% EtOH for at least 12 h followed by MilliQ H_2O for at least 12 h to remove any unreacted monomers. Hydrogel disks of a 4 mm diameter were punched out of the hydrogel slab with a cork borer.

2.3 Thermal and photothermal behavior of hydrogel-nanoshell composites

After synthesis, the swelling behavior of the poly(NIPAAm-co-AAm) hydrogels was analyzed in response to temperature. The hydrogels were allowed to swell at room temperature (22 °C) for at least 24 h before testing. To determine the LCST of the hydrogels, the hydrogels were first weighed and placed in TRIS buffer (pH 7.4), and then incubated at various temperatures (29 °C, 33 °C, 37 °C, 41 °C, 45 °C, and 50 °C) for 10

min. Deswelling ratio (DSR) was calculated as follows: $DSR = 100 * Weight_{Temp} / Weight_{Temp=22°C}$.

Next, the thermal behaviors of hydrogels with and without nanoshells were compared. The hydrogels were placed in 2 ml TRIS buffer (pH 7.4) and incubated for 30 min in a 50°C water bath or exposed to an NIR diode laser (Coherent; Santa Clara, CA) at 808 nm, 8 W/cm^2 for 30 min. Deswelling ratio was calculated as follows: $DSR = 100 * Weight_t / Weight_{t=0}$.

2.4 Loading and release of cancer therapeutics

Hydrogels with and without nanoshells were dried under vacuum for at least 48 h prior to drug loading. The dry weights of the hydrogels were recorded. One set of hydrogels was then soaked in a 0.5 mg/ml (862 μM) solution of doxorubicin (Sigma-Aldrich; St. Louis, MO) in TRIS buffer (pH 7.4) at 4°C for 24 h. Absorbance readings of loaded hydrogels at 485 nm were used to determine the loaded concentration of doxorubicin, with absorbance readings of non-drug loaded hydrogels used as blanks. A separate set of hydrogels was soaked in a 17 μM (0.22 mg/ml) solution of a 21-bp DNA duplex (Integrated DNA Technologies, inc.) in duplex buffer (30 mM HEPES, 100 mM potassium acetate, pH 7.5) (Integrated DNA Technologies, inc.) at 4°C for 24 h. DNA duplex loading was estimated by measuring the concentration of the soak solution before and after hydrogel soaking.

Loaded hydrogels, both with and without nanoshells, were placed in TRIS buffer (doxorubicin hydrogels) or duplex buffer (DNA duplex hydrogels) and then exposed to an NIR diode laser (Coherent) at 808 nm, 8 W/cm^2 for 30 min. In addition, control hydrogels with nanoshells were kept at room temperature (22°C) for 30 min to evaluate release due to passive diffusion. Every 5 min, a buffer sample was analyzed for drug content via absorbance measurements (doxorubicin, 485 nm; DNA, 260 nm). Release profiles from these three groups were analyzed using a one-way ANOVA with Tukey's post-hoc test.

2.5 Delivery of doxorubicin to CT26.WT cells

Murine colon carcinoma cells (CT-26.WT cells, ATCC) were cultured in RPMI 1640 media (ATCC) supplemented with 2 mM L-glutamine, 10 mM HEPES, 1 mM sodium pyruvate, 4.5 g/L glucose, 1.5 g/L sodium bicarbonate, 1% penicillin, 1% streptomycin, and 10% fetal bovine serum (FBS). Cultures were maintained at 37 °C with 5% CO_2.

Cells were seeded in fibronectin-coated 24-well culture plates at a density of 75,000 cells/ml. After 24 h, a doxorubicin-loaded composite hydrogel or a non-loaded composite hydrogel was placed in a transwell insert (PET membrane, 0.4 μm pore size, BD) and covered with media. The hydrogels were then exposed to the NIR laser (808 nm, 8 W/cm^2, 10 min) after which the hydrogel and insert were removed and the cells were incubated for an additional 24-48 h. Additional groups included cells that were exposed to loaded composite hydrogels for both 10 min (equivalent time as NIR exposure) and 24 h as controls, as well as cells which were exposed to 5.4 μg of free dox/well (approximately the amount of doxorubicin that was released from one gel following 10 min of irradiation). After 24 hours, cellular uptake of doxorubicin was assayed by fluorescent microscopy (560

nm excitation, 645 nm emission) using an Axiovert 135 inverted fluorescent microscope (Zeiss). Doxorubicin fluorescent intensity was quantified using ImageJ (NIH) and analyzed using a Student's t-test with a 95% confidence interval. After 48 h, cell proliferation was assessed using a CellTiter96® AQueous proliferation assay (Promega). Cell viability was normalized to the viability of non-treated cells.

3 Results

3.1 Hydrogel-nanoshell composite characterization

As synthesized, the nanoshells utilized in this study were found to have a diameter of 153 ± 9 nm (as analyzed by TEM) and a Z-average diameter of 156.0 nm and a polydispersity index of 0.090 (as analyzed by DLS). These particles strongly absorb in the near infrared, with a peak extinction coefficient at 780 nm. A TEM image of the gold-silica nanoshells and their extinction spectra are shown (Fig. 1).

The poly(NIPAAm-co-AAm) hydrogels collapse in a temperature range from 39-45°C (Fig. 2). This indicates the potential for this material to be used as a depot for drug molecules under physiological conditions, as the material is in a highly swollen state at 37 °C, but a highly collapsed state at 40-45 °C. Next, we demonstrate the ability of the thermal phase transition to be triggered by the encapsulated nanoshells. Hydrogels with and without nanoshells displayed similar behavior when incubated at 50°C, indicating that the presence of nanoshells did not inhibit hydrogel collapse (Fig. 2). When exposed to NIR light, the nanoshells heated and elicited a temperature increase of surrounding material, resulting in hydrogels with nanoshells deswelling similarly to the hydrogels incubated at 50°C in the water bath. Hydrogels without nanoshells exhibited minimal deswelling in response to the laser, demonstrating that both the presence of nanoshells and exposure to an NIR laser were required to cause hydrogel deswelling in response to NIR light.

3.2 Loading and release of cancer therapeutics

In separate studies, a chemotherapeutic (doxorubicin) and a biologic therapy (dsDNA) were passively absorbed into the material, with amounts of drug loaded shown in Table 1. Release of the drug followed exposure to NIR irradiation (Fig. 3).

Doxorubicin delivery after NIR irradiation indicated that nanoshell-composites provide increased release over controls for all times $t > 0$ (Fig. 3A). After 30 min, delivery of doxorubicin from the irradiated composite hydrogels was approximately 2 times higher than irradiation of hydrogels without nanoshells. (329 μg/g compared to 158 μg/g). Delivery of dsDNA delivery from irradiated composites was nearly 5 times higher than irradiated hydrogels without nanoshells (197.8 μg/g vs 39.68 μg/g) after 30 minutes (Fig. 3B). Overall, 71% of loaded doxorubicin was released from the composite hydrogels after 30 minutes of irradiation, compared to 93% loaded dsDNA. In a separate study using doxorubicin-loaded composite hydrogels, NIR light exposure was cycled on and off over a 30 min period (10 min off, 10 min on, 10 min off) to further demonstrate the dependence of release kinetics on NIR exposure.

3.3 Delivery of doxorubicin to CT26-WT Cells

To evaluate cellular uptake and biological efficacy, doxorubicin was released from these hydrogel composites and allowed to act on cultured colon carcinoma cells. After 24 hours, cell exposed to irradiated hydrogels showed increased intracellular doxorubicin as compared to cells exposed to non-irradiated hydrogels(Fig. 4A-C). Cells that were exposed to the irradiated hydrogels containing doxorubicin showed a 30% decrease in proliferation (Fig. 4D) in response to doxorubicin exposure, whereas cells cultured with a non-irradiated doxorubicin composite exhibited minimal changes in proliferation, indicating that the loaded doxorubicin was available to cells only when hydrogels were forced to undergo a phase transition. Further, cells exposed to free doxorubicin showed a similar decrease in proliferation as was seen in the irradiated composite group. Cells exposed to irradiated gels that were not loaded with drug did not exhibit any decrease in proliferation.

4 Discussion

The goal of this work was to design and investigate materials for an optically-triggered cancer therapeutic delivery platform. Materials used in such a platform need to act to (1) encapsulate a therapeutic cargo to limit tissue exposure before desired delivery, and (2) trigger release of this cargo at a specific time and location. The first goal was accomplished by the utilization of a thermally-responsive poly(NIPAAm-co-AAm) hydrogel. This material acts similarly to a sponge, allowing therapeutic molecules to be absorbed within its pores. In addition, this hydrogel was found to have an LCST slightly above 37 °C, thereby existing in a swollen state at human body temperature, but going through the desired phase change at temperatures easily achievable with minimal biological consequences.

The second goal, triggering the phase transition, was accomplished by the encapsulation of gold-silica nanoshells within the hydrogel. When exposed to light in the NIR range, the nanoshells elicited a temperature increase of the surrounding material. This caused the hydrogel material to collapse and rapidly expel large amounts of water and absorbed therapeutic, demonstrating the capability of optically triggering this material phase transition and subsequent drug delivery.

The loading and release of this therapeutics from the system showed some differing characteristics. For loading of both doxorubicin and dsDNA, a higher amount of drug could be loaded into the composite hydrogels with nanoshells compared to the polymer-only hydrogels. Overall, a higher concentration of doxorubicin (836 μM) was loaded into the hydrogels than the DNA duplexes (17 μM). This is because doxorubicin is a much smaller molecule, and can therefore easily diffuse into the hydrogel material during loading. However, this same property causes doxorubicin to passively diffuse out of the material much faster than the DNA, leading to higher levels of non-triggered delivery (158 μg/g gel doxorubicin release seen at room temperature vs 40 μg/g dsDNA release). In addition, despite its small size, an overall lower percentage of doxorubicin delivery is seen over 30 min when compared to dsDNA (71% doxorubicin delivered following irradiation, as compared to 93% dsDNA delivered). This is likely due to the chemical nature of the therapeutic being delivered. Hydrophillic molecules are more advantageous for this system, as the material phase transition is based upon the hydrophobic effect, with the hydrophobic

polymer material phase separating from its aqueous environment. Therapeutics molecules that are more hydrophobic will have increased affinity to the polymer material, causing them to remain encapsulated within the hydrogel material following water expulsion.

While this study clearly demonstrates that a molecule similar to siRNA can be efficiently delivered out of the composite material, a nucleic acid therapy must then be internalized into cells to be effective. In future studies, efficient cellular uptake and subsequent changes in gene or protein expression due to the delivered nucleic acid therapy should be investigated. Improving siRNA transport into cells is an active area of research today [29]. Several studies have shown that modification of siRNA molecules with small chemical groups greatly enhances cellular uptake and efficacy [30,31], and we hypothesize that the incorporation of such small chemical groups to improve siRNA cellular uptake efficiency would not significantly influence release kinetics from our composite material.

These studies validate the potential for this composite material to be used for controlled delivery of cancer therapeutics. Towards translation of this material into *in vivo* applications, the composites could be synthesized as injectable-sized particles rather than bulk discs. This would allow for a platform of similar size as liposomal drug formulations, thus allowing for passive targeting of intravenously administered particles to tumor tissue due to the enhanced permeation and retention effect [32]. After accumulation of particles in tumor tissue, release of drug from the carrier would then be triggered by external NIR exposure.

This platform also has the inherit ability to cause cancer necrosis by two mechanisms simultaneously. The encapsulated nanoshells can be used to generate sufficient heating to cause tissue necrosis, as well as allow for a burst release of cytotoxic payload. Further, numerous studies have shown increased benefits of chemotherapeutic treatments when combined hyperthermic treatments as well [33–35]. In fact, combining hyperthermia and chemical drugs has been shown to elicit a more than additive response for multiple classes of chemotherapeutic agents, including platinum drugs, alkylating agents, nitrosources, and antibiotics [36].

Additionally, we have demonstrated the ability of this material to deliver a range of molecules, from small chemical drugs to large biologic therapeutics. It is the norm for most patients is to receive a cocktail of many different drugs rather than a single agent since combinations of drugs with different mechanisms of action show benefit in preventing drug resistant tumor cells [37]. It is conceivable that this material could be loaded with multiple chemical therapeutics for delivery to a patient. For example, much research has been done showing an increased benefit of combining siRNA therapy with a chemotherapeutic such as doxorubicin, especially for multi-drug resistant cancers [38–41]. The versatility of this platform for use with multiple types of therapeutics would allow for an ease of implementation of such regimens.

5 Conclusions

The ability to precisely control therapeutic delivery to malignant tissue would undoubtedly improve cancer management by overcoming limitations of current therapies. The controlled

release system designed in this report would decrease the off-site toxicities of systemic chemotherapeutic regimens by minimizing drug exposure to non-malignant tissue, as well as increase the serum stability of fragile biologic therapeutics. The poly(NIPAAm-co-AAm)-gold nanoshell composites were loaded with cancer therapeutics, and their release was optically-triggered. Ultimately, this material could be used to create a platform that would attack tumor tissue using two distinct mechanisms simultaneously: (1) photothermal heating, (2) delivery of multiple types of therapeutic molecules, providing a novel approach to effectively treat cancers when standard treatment modalities are not adequate.

Supplementary Material

Refer to Web version on PubMed Central for supplementary material.

References

1. Kikuchi A, Okano T. Pulsatile drug release control using hydrogels. Adv. Drug Deliv. Rev. 2002; 54:53–77. [PubMed: 11755706]
2. Brabant G, Prank K, Schofl C. Pulsatile patterns in hormone secretion. Trends Endocrinol. Metab. 1992; 3:183–190. [PubMed: 18407099]
3. Smolensky MH, Peppas NA. Chronobiology, drug delivery, and chronotherapeutics. Adv. Drug Deliv. Rev. 2007; 59:828–51. [PubMed: 17884237]
4. Eriguchi M, Levi F, Hisa T, Yanagie H, Nonaka Y, Takeda Y. Chronotherapy for cancer. Biomed. Pharmacother. 2003; 57:92–95.
5. Siegel R, DeSantis C, Virgo K, Stein K, Mariotto A, Smith T, et al. Cancer treatment and survivorship statistics. CA Cancer J. Clin. 2012; 2012; 62:220–41. [PubMed: 22700443]
6. Lévi F, Zidani R, Misset JL. Randomised multicentre trial of chronotherapy with oxaliplatin, fluorouracil, and folinic acid in metastatic colorectal cancer. Lancet. 1997; 350:681–6. [PubMed: 9291901]
7. Strong LE, West JL. Thermally responsive polymer-nanoparticle composites for biomedical applications. Wiley Interdiscip. Rev. Nanomed. Nanobiotechnol. 2011; 3:307–17. [PubMed: 21384563]
8. Bikram M, West JL. Thermo-responsive systems for controlled drug delivery. Expert Opin Drug Delv. 2008; 5:1077–91.
9. Yoshida R, Sakai K, Okano T, Sakurai Y. Modulating the phase transition temperature and thermosensitivity in N-isopropylacrylamide copolymer gels. J. Biomater. Sci. Polym. Ed. 1995; 6:585–598. [PubMed: 7873510]
10. Sershen S, Westcott S, Halas N, West J. Temperature-sensitive polymer-nanoshell composites for photothermally modulated drug delivery. J. Biomed. Mater. Res. 2000; 51:293–298. [PubMed: 10880069]
11. Bikram M, Gobin AM, Whitmire RE, West JL. Temperature-sensitive hydrogels with SiO2-Au nanoshells for controlled drug delivery. J. Control Release. 2007; 123:219–27. [PubMed: 17920154]
12. Oldenburg S. Nanoengineering of optical resonances. Chem. Phys. Lett. 1998; 288:243–247.
13. Averitt RD, Westcott SL, Halas NJ. Linear optical properties of gold nanoshells. J. Opt. Soc. Am. B. 1999; 16:1824–32.
14. Daniel M-C, Astruc D. Gold nanoparticles: assembly, supramolecular chemistry, quantum-size-related properties, and applications toward biology, catalysis, and nanotechnology. Chem. Rev. 2004; 104:293–346. [PubMed: 14719978]
15. Averitt RD, Westcott SL, Halas NJ. Ultrafast optical properties of gold nanoshells. J. Opt. Soc. Am. B. 1999; 16:1814–23.
16. Weissleder R. A clearer vision for in vivo imaging. Nat. Biotechnol. 2001; 19:316–317. [PubMed: 11283581]

17. Hirsch LR, Gobin AM, Lowery AR, Tam F, a Drezek R, Halas NJ, et al. Metal nanoshells. Ann. Biomed. Eng. 2006; 34:15–22. [PubMed: 16528617]
18. Hirsch L, Jackson J, Lee A, Halas N, West J. A whole blood immunoassay using gold nanoshells. Anal. Chem. 2003; 75:2377–81. [PubMed: 12918980]
19. Loo C, Hirsch L, Lee M-H, Chang E, West J, Halas N, et al. Gold nanoshell bioconjugates for molecular imaging in living cells. Opt. Lett. 2005; 30:1012–4. [PubMed: 15906987]
20. Loo C, Lowery A, Halas N, West J, Drezek R. Immunotargeted nanoshells for integrated cancer imaging and therapy. Nano Lett. 2005; 5:709–11. [PubMed: 15826113]
21. Loo C, Lin A, Hirsch L, Lee M-H, Barton J, Halas N, et al. Nanoshell-enabled photonics-based imaging and therapy of cancer. Technol. Cancer Res. Treat. 2004; 3:33–40. [PubMed: 14750891]
22. Rubin, P. 8th ed.. W.B. Saunders Company; Philadelphia, PA: 2001. Clinical Oncology: A Multidisiplinary Approach for Physicians and Students.
23. Fornari FA, Randolph JK, Yalowich JC, Ritke MK, Gewirtz DA. Interference by doxorubicin with DNA unwinding in MCF-7 breast tumor cells. Mol. Pharmacol. 1994; 45:649–56. [PubMed: 8183243]
24. Saltiel E, McGuire W. Doxorubicin (adriamycin) cardiomyopathy. West. J. Med. 1983; 139:332–41. [PubMed: 6356608]
25. Duxbury MS, Ito H, Zinner MJ, Ashley SW, Whang EE. EphA2: a determinant of malignant cellular behavior and a potential therapeutic target in pancreatic adenocarcinoma. Oncogene. 2004; 23:1448–56. [PubMed: 14973554]
26. Gale NW, Yancopoulos GD. Growth factors acting via endothelial cell-specific receptor tyrosine kinases: VEGFs, angiopoietins, and ephrins in vascular development. Genes Dev. 1999; 13:1055–66. [PubMed: 10323857]
27. Landen CN, Chavez-Reyes A, Bucana C, Schmandt R, Deavers MT, Lopez-Berestein G, et al. Therapeutic EphA2 gene targeting in vivo using neutral liposomal small interfering RNA delivery. Cancer Res. 2005; 65:6910–8. [PubMed: 16061675]
28. Duff DG, Baiker A, Edwards PP. A new hydrosol of gold clusters. 1. Formation and particle size variation. Langmuir. 1993; 9:2301–2309.
29. Oh Y-K, Park TG. siRNA delivery systems for cancer treatment. Adv. Drug Deliv. Rev. 2009; 61:850–62. [PubMed: 19422869]
30. Bramsen JB, Laursen MB, Nielsen AF, Hansen TB, Bus C, Langkjaer N, et al. A large-scale chemical modification screen identifies design rules to generate siRNAs with high activity, high stability and low toxicity. Nucleic Acids Res. 2009; 37:2867–81. [PubMed: 19282453]
31. Mook O, Vreijling J, Wengel SL, Wengel J, Zhou C, Chattopadhyaya J, et al. In vivo efficacy and off-target effects of locked nucleic acid (LNA) and unlocked nucleic acid (UNA) modified siRNA and small internally segmented interfering RNA (sisiRNA) in mice bearing human tumor xenografts. Artif. DNA PNA XNA. 2010; 1:36–44. [PubMed: 21687525]
32. Matsumura Y, Maeda H. A New Concept for Macromolecular Therapeutics in Cancer Chemotherapy: Mechanism of Tumoritropic Accumulation of Proteins and the Antitumor Agent Smancs. Cancer Res. 1986; 46:6387–92. [PubMed: 2946403]
33. Hildebrandt B. The cellular and molecular basis of hyperthermia. Crit. Rev. Oncol. Hematol. 2002; 43:33–56. [PubMed: 12098606]
34. Hahn GM. Potential for therapy of drugs and hyperthermia. Cancer Res. 1979; 39:2264–8. [PubMed: 87263]
35. Marmor JB. Interactions of hyperthermia and chemotherapy in animals. Cancer Res. 1979; 39:2269–76. [PubMed: 87264]
36. Issels RD. Hyperthermia adds to chemotherapy. Eur. J. Cancer. 2008; 44:2546–54. [PubMed: 18789678]
37. Chabner BA, Roberts TG. Timeline: Chemotherapy and the war on cancer. Nat. Rev. Cancer. 2005; 5:65–72. [PubMed: 15630416]
38. Lima RT, Martins LM, Guimarães JE, Sambade C, Vasconcelos MH. Specific downregulation of bcl-2 and xIAP by RNAi enhances the effects of chemotherapeutic agents in MCF-7 human breast cancer cells. Cancer Gene Ther. 2004; 11:309–16. [PubMed: 15031723]

39. Dong X, Liu A, Zer C, Feng J, Zhen Z, Yang M, et al. siRNA inhibition of telomerase enhances the anti-cancer effect of doxorubicin in breast cancer cells. BMC Cancer. 2009; 9:133–43. [PubMed: 19416503]

40. Meng H, Liong M, Xia T, Li Z, Ji Z, Zink JI, et al. Engineered design of mesoporous silica nanoparticles to deliver doxorubicin and P-glycoprotein siRNA to overcome drug resistance in a cancer cell line. ACS Nano. 2010; 4:4539–50. [PubMed: 20731437]

41. Xiong X-B, Lavasanifar A. Traceable Multifunctional Micellar Nanocarriers for Cancer-Targeted Co-delivery of MDR-1 siRNA and Doxorubicin. ACS Nano. 2011:5202–5213. [PubMed: 21627074]

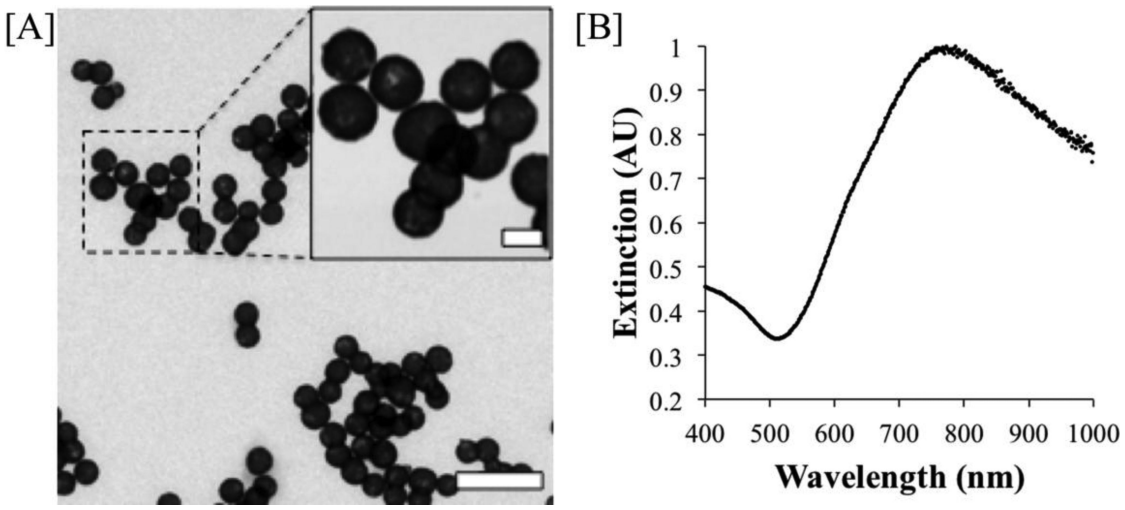

Figure 1. Gold-silica nanoshell characterization

[A] TEM image of synthesized gold-silica nanoshells. (Scale bars = 500 nm, 100 nm inset) shows a uniform population of particles with a diameter of ~150 nm. [B] Extinction spectra of synthesized gold-silica nanoshells with a peak at 780 nm.

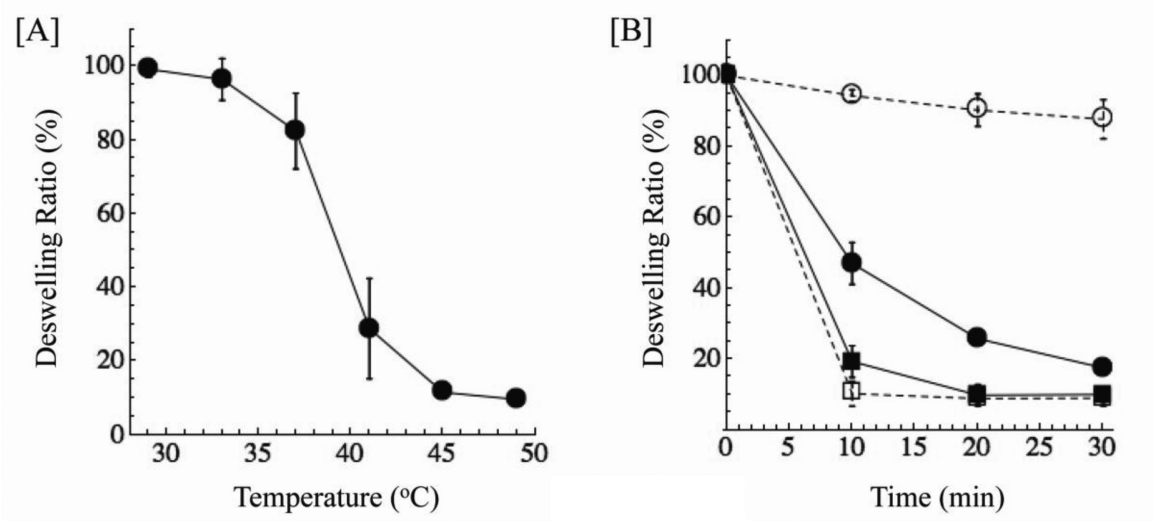

Figure 2. Characterization of poly(NIPAAm-co-AAm) hydrogels

[A] Deswelling of poly(NIPAAm-co-AAm) hydrogels as a function of temperature. These hydrogels collapse from 39-45 °C, slightly above human physiological temperature. [B] Deswelling of NIPAAm-co-AAm hydrogels with (solid lines) and without (dashed lines) nanoshells by either incubation in a 50 °C water bath (squares) or exposure to a NIR laser (808 nm, 8 W/cm^2) (ciricles). Both materials displayed similar deswelling behaviors when incubated above material LCST, while only hydrogels with the nanoshells showed deswelling in response to NIR irradiation.

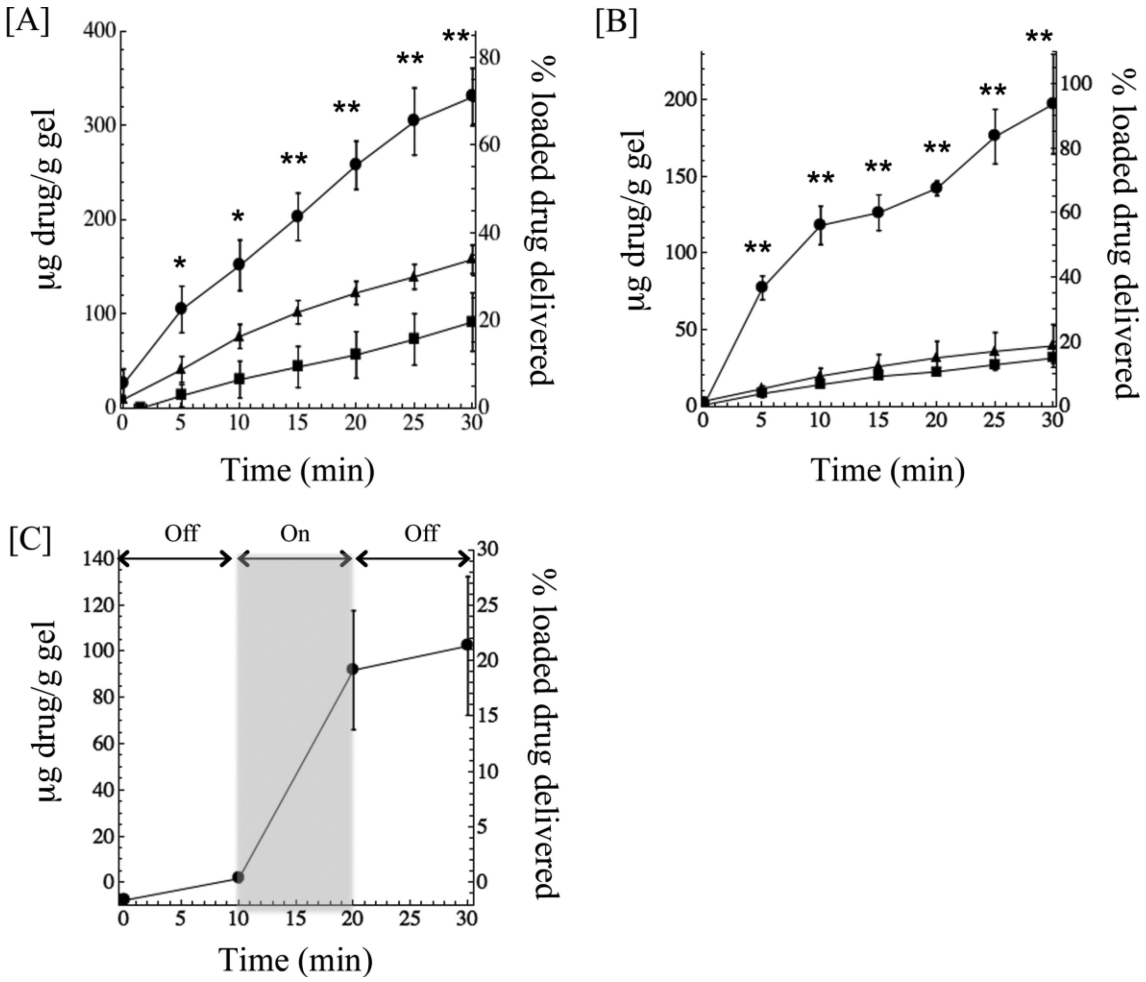

Figure 3. Release of doxorubicin and DNA duplexes from poly(NIPAAm-co-AAm)-nanoshell composite hydrogels

Release of [A] doxorubicin and [B] DNA duplexes from composite hydrogels. Gels containing nanoshells exposed to an 808 nm laser at 8 W/cm^2 (circles) delivered significantly more drug than gels without nanoshells exposed to the same laser settings (triangles) and gels with nanoshells left at room temperature as a control (squares). *$p<0.05$, **$p<0.01$, as compared to irradiation without nanoshells. [C] Delivery of doxorubicin from composite hydrogels exposed to cyclic NIR irradiation (10 min off, 10 min on, 10 min off) shows that the rate of release from the composite greatly increases in response to NIR exposure.

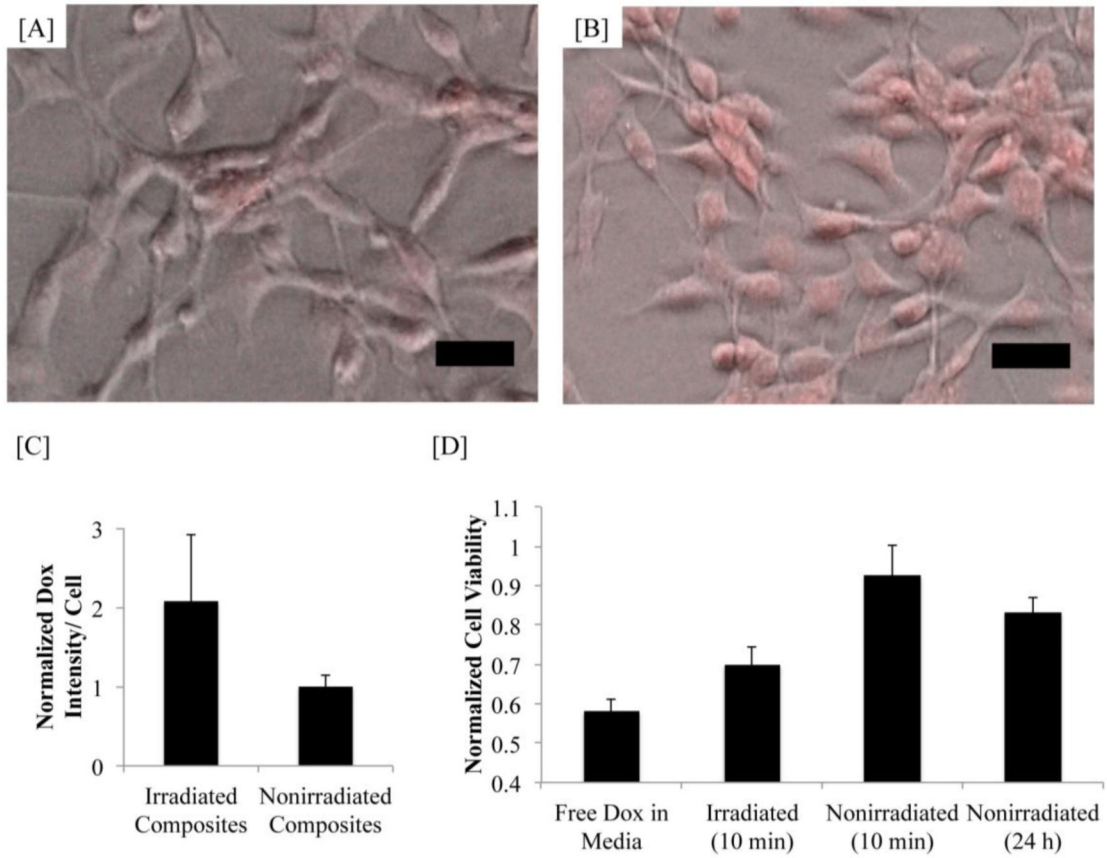

Figure 4. Doxorubicin delivery to CT26-WT cells

[A] Phase images overlayed with doxorubicin fluorescent signal of cells exposed to irradiated composite hydrogels [A] and non-irradiated composite hydrogels [B]. Scale bars = 50 μm. [C] Quantification of intracellular doxorubicin fluorescence. Cells exposed to irradiated gels have a significantly higher doxorubicin signal than cells exposed to non-irradiated gels ($p<0.05$). [D] Changes in cell viability due to doxorubicin delivery from composite gels. Cells exposed to irradiated gels showed a significant decrease in viability ($p<0.05$) compared to cells exposed to non-irradiated gels, even approaching the response of cells exposed to free doxorubicin.

Table 1

Drug Loading of Hydrogel Composites.

With Nanoshells		Without Nanoshells		
Doxorubicin	**dsDNA**	**Doxorubicin**	**dsDNA**	
466.5 ± 2.6	221.0 ± 13.1	418.3 ± 5.1	209.7 ± 0.9	μg drug loaded / g gel
17.4 ± 1.7	9.0 ± 0.5	15.6 ± 2.0	6.6 ± 0.6	μg of drug per 4 mm hydrogel disk